Simulation of a Novel Junction-less Solar Cell Structure Using PC-1D Software

Khaled M. Dadesh, and Wafa S. Alarabi

Electric and Electronic Engineering Department, University of Tripoli, Tripoli, Libya

Email: k.dadesh@uot.edu.ly, eng.wafa.alarabi@gmail.com

Abstract: The continues demand for Photovoltaic device improvement has led us to search for new sources of photovoltaic action. For that, this paper proves the existence of other sources for photovoltaic action in addition to the main source which is the built-in electrostatic field generated through controlled composition gradient

Those new sources are uncovered through mathematical examination of a specific material system followed by the construction of four-layer p-type semi-conducting materials (i.e., without pn-junction formation). First three layers of this specific material system are fabricated with $Al_xGa_{1-x}As$ with different Aluminum fractions, while the fourth layer is fabricated with Ge with a diffused back surface field (BSF) layer to reduce surface recombination velocities (SRV).

The complete structure is analyzed using the PC-1D simulation software, and it shows that the junction-less structure possesses the photovoltaic action with low performance.

محاكاة لبنية خلية شمسية جديدة بلا وصلة بإستخدام برمجية PC-1D

خالد محمد ددش * و وفاء سالم العربي

قسم الهندسة الكهربائية والالكترونية ـ كلية الهندسة ـ جامعة طرابلس. طرابلس ـ ليبيا

ملخص: الحاجة المستمرة لتحسين كفاءة الخلايا الكهروضوئية أدى للبحث عن مصادر جديدة لظاهرة التأثير الكهروضوئي تعمل بها تلك الخلايا، لهذا تُناقش هذه الورقة البحثية الكشف عن مصادر إضافية للتأثير

* Corresponding author

الكهروضوئي -بالإضافة للمصدر الرئيسي وهو المجال الكهربائي المتكون عند الوصلة (وصلة بي-إن)- ناتج عن عملية تشويب (تطعيم) تدريجي في بنية الخلية.

تم الكشف عن هذه المصادر بالتحليل الرياضي لبنية معينة من المواد متبوعاً بمحاكاة لخلية شمسية مكونة من أربع طبقات من أشباه الموصلات الموجبة فقط (أي لا وجود لشبه موصل سالب و بالتالي عدم تكون وصلة بي-إن التقليدية). الطبقة الأولى و الثانية و الثالثة في البنية التي ندرسها في هذه الورقه مكونة من زرنيخيد (أرسينيد) الألومنيوم والغاليوم بنسب مختلفة من أرسينيد الألومنيوم لكل طبقة، بينما تتكون الطبقة الرابعة من الجرمانيوم مع تكوين طبقة حقل خلفي للتقليل من سرعة إعادة التركيب السطحي والتقليل من تشتت حاملات الشحنة نحو الوصلة.

تم تحليل البنية الكاملة بإستخدام برنامج المحاكاة PC-1D الذي أظهر وجود ظاهرة التأثير الكهروضوئي في الخلايا عديمة الوصلة.

.

Keywords: *Junction-less solar cells, Photovoltaic sources, uniform gradient doping, Dember potential, PC1D.*

1. INTRODUCTION

In 1839, the French scientist, Alexander-Edmond Becquerel discovered the photoelectric effect through an experiment with an electrolytic cell made up of an electrode (platinum) and an electrolyte (silver chloride) placed in an electricity-conducting solution. He found that electricity-generation increases upon exposure to light. In 1883 the first photovoltaic device was invented by the American inventor Charles Fritts who described the first solar cells made from selenium wafers. In 1939 The first photovoltaic device using a Si p-n junction was built by Russell Ohl. [1].

The development of solar technology has continued and the pace towards low cost and high efficiency solar cells is non-stop [2].

The operation of most developed solar cells mainly lies on the existence of built-in potential in the pn-junction [3]. Taking this fact in consideration, some trends have worked on optimizing the key parameters of single junction solar cells [4], some trends have gone to develop multi-junction solar cells in order to increase the collection probabilities of photo-generated carriers [5], and others trends have gone to multi-junction solar cells fabricated with multiple semiconductor layers (sub-cells) to produce electricity at higher operating efficiencies, where each layer has it's unique band gap designed to efficiently absorb a specific segment of the solar spectrum [6]. High efficiencies can be also obtained through the design of complicated textured surfaces or multi-layer anti-reflecting coatings [7]. In addition, some have worked on developing high-efficiency concentrated solar cells [8].

However, in all those solar cells whether they're single layer- single pn- junction cells or alternating pn-pn multi-layer cells, the common property among all that the pn-junction formation is basic, while in our work the pn-junction formation is excluded

Our approach takes in consideration the energy band gap engineering [9] seeking to develop a new solar cell design that utilizes the theory that capitalizes the gradient in the energy band diagram. This gradient is made by cascading similar p-type or n-type material with different energy-gap materials to create an electric field along the device structure. This field will be the main source of the photovoltaic action or effect. This theory was mainly developed by Stephen J. Fonash since 1981 [10].

In this paper we'll basically uncover other possible sources of photovoltaic action trough mathematical examination and computer simulation of a specific material system. Then we will construct a multi-layer junction-less solar cell which will be constructed of a p-type semiconductor only.

As production costs of solar cells are very high, software packages are always used to simulate any possible architecture before physical production in order to study what power output can be obtained with different input parameters. PC-1D software will be used to simulate our proposed structure.

2. MATHEMATICAL ANALYSIS

Fonash started his theory proof by mathematical examination of a general material system shown in Figure 1. To keep his exploration as general as possible, he allowed the semiconductor-electron affinity χ, band gab Eg, and band effective densities of states Nc and Nυ to be functions of positions while the precise dependence of built-in electrostatic field on the position will not be specified. Furthermore, semiconductor type will not be specified. He also assumed that there are no temperature gradients present and all carriers are taken to be at the lattice temperature.
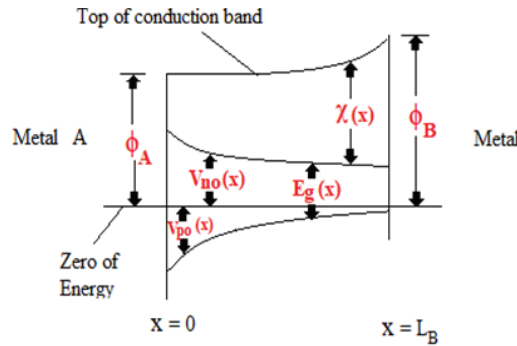
(a)
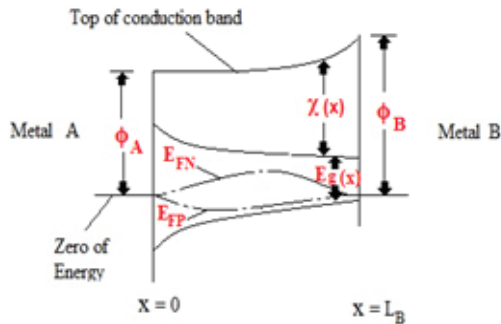
(b)

Figure 1. A very general semiconductor material located between two ohmic contacts. (a) at thermodynamic equilibrium. (b) under illumination.

In the materials system shown above, Ohmic contacts exist at both ends of this materials system [11]. Thus, the difference in Fermi-level positions of metal A and B of Figure.1, under illumination with the structure open-circuited, will give an open circuit voltage V_{oc} where:

φA: the work function of metal A

φB : the work function of metal B

χ: Electron affinity

Vn: Energy difference between the conduction band edge and the electron quasi-Fermi level

Vp: Energy difference between the hole quasi-Fermi level and the valence-band edge

The V_{oc} will be computed for the above general configuration to determine all possible sources of photo-voltage. Fonash assumed that any electron and hole transport present in the structure takes place in the valence and conduction bands only. Consequently, the attention is focused on the expressions of J_n and J_p which are given by:

$$J_n = e\mu_n n\left[\zeta - \frac{d\chi}{dx} - KT\frac{d}{dx}\ln N_c\right] + eD_n\frac{dn}{dx}$$ .... (1)

$$J_p = e\mu_p p\left[\zeta - \frac{d}{dx}(\chi + E_g) + KT\frac{d}{dx}\ln N_v\right] - eD_p\frac{dp}{dx}$$ .... (2)

Written in terms of the quasi-Fermi level E_{Fn} for electrons and the quasi-Fermi level E_{Fp} for holes, J_n and J_p become:

$$J_n = e\mu_n n(dE_{Fn}/dx)$$ .... (1.a)

$$J_p = e\mu_p p(dE_{Fp}/dx)$$ .... (2.a)

As shown in Fig. 1.a, under thermodynamic equilibrium and .

It is also known that:

$$n_0 = N_c e^{-V_{n0}/KT}$$ .... (3)

From Eqs. (1)-(4) and the fact that $J_n = J_p = 0$ under thermodynamic equilibrium, an expression for the built-in electrostatic field $\xi_0 = \xi_0(x)$ can be obtained as:

$$p_0 = N_v e^{-V_{p0}/KT}$$ .... (4)

$$\xi_0 = \frac{d\chi}{dx} + \frac{dV_{no}}{dx} = -\frac{dV_{po}}{dx} + \frac{dE_g}{dx} + \frac{d\chi}{dx}$$ .... (5)

Once the structure is illuminated it is driven out of its thermodynamic equilibrium state and Figure 1.b applies. The electrostatic field will no longer be $\xi_0 = \xi_0(x)$, but it l becomes $\xi = \xi(x)$.

$$\xi_0 = \frac{d}{dx}(E_{Fn} - V_n + \chi) = \frac{d}{dx}(E_{Fp} - V_p + E_g + \chi)$$ .... (6)

Hence, V_{oc} can be computed by:

$$V_{oc} = \int_0^L (\xi - \xi_0)dx$$ .... (7)

Evaluating this integral results in a catalog displaying the various sources of photovoltaic action

$$V_{oc} = -\int_0^L \left(\frac{e\mu_n\Delta p + e\mu_p\Delta p}{\sigma}\right)\xi_0 dx + \int_0^L \left(\frac{e\mu_n\Delta n}{\sigma}\right)\frac{d\chi}{dx}dx + \int_0^L \left(\frac{e\mu_p\Delta p}{\sigma}\right)\left(\frac{d\chi}{dx} + \frac{dE_g}{dx}\right)dx$$
$$- KT\int_0^L \left(\frac{e\mu_p\Delta p}{\sigma}\frac{d}{dx}\ln N_v - \frac{e\mu_n\Delta n}{\sigma}\frac{d}{dx}\ln N_c\right)dx$$
$$+ KT\int_0^L \frac{1}{\sigma}\left(e\mu_p\frac{d}{dx}\Delta p - e\mu_n\frac{d}{dx}\Delta n\right)dx$$ .... (8)

We can have an alternative expression for equation (8) by using these expressions:

$$dE_c/dx = \xi_0 - d\chi/dx \quad\text{..}\quad (9)$$

$$dE_v/dx = \xi_0 - d(E_g + \chi)/dx \quad\text{...}\quad (10)$$

These expressions relate the derivatives of the band edges to the electrostatic field and to the gradient in the electron affinity χ and the hole affinity $E_g + \chi$. Equations (9) and (10) follow from the fact that the top of the conduction band is reached either by adding χ to E_c or by adding $\chi + E_g$ to at any point in a semiconductor.

Equation (8) also uses $n = \Delta n + n_0$ and $p = \Delta p + p_0$ as well as $\sigma = \Delta\sigma + \sigma_0$. Δn and Δp are light-induced changes in population, and the quantity σ is the total conductivity in the presence of light. It is larger than the thermodynamic equilibrium value σ_0 by the light-induced change $\Delta\sigma$.

So, equation (8) becomes:

$$
\begin{aligned}
V_{oc} = &-\int_0^L \left(\frac{e\mu_n \Delta n}{\sigma}\right)\frac{dE_g}{dx}dx - \int_0^L \left(\frac{e\mu_p \Delta p}{\sigma}\right)\frac{dE_v}{dx}dx \\
&- KT\int_0^L \left(\frac{e\mu_p \Delta p}{\sigma}\frac{d}{dx}\ln N_v - \frac{e\mu_n \Delta n}{\sigma}\frac{d}{dx}\ln N_c\right)dx \\
&+ KT\int_0^L \frac{1}{\sigma}\left(e\mu_p \frac{d}{dx}\Delta p - e\mu_n \frac{d}{dx}\Delta n\right)dx \quad\text{..............................}\quad (11)
\end{aligned}
$$

However, in either cases equation (8) provides a useful catalog of possible sources of photovoltaic action.

Focusing on the Equation we see that the built-in electrostatic field ξ is, indeed, a source of photo-voltage, but we also clearly see that effective forces arising from electron and hole affinity variations and band effective density of states variations are also sources of photo-voltage, also there is a contribution of the form :

$$KT\int_0^L \frac{1}{\sigma}\left(e\mu_p \frac{d}{dx}\Delta p - e\mu_n \frac{d}{dx}\Delta n\right)dx$$

Which has been uncovered as a result of the exploration. This component of the photo-voltage is termed as the Dember potential.

Eventually, Fonash's theory proves that the photovoltaic action in a solar cell structure can arise from the presence of an Electrostatic field, effective force fields due to material property variation and Dember potential.

Taking in consideration all mathematical analytics and physical concepts that have been discussed, we will construct a multi-layer solar cell made of a P-type semiconductor only using PC1D software to prove that a photovoltaic action could be produced through such structure.

3. PC-1D JUNCTION-LESS SOLAR CELL IMPLEMENTATION

Our proposed structure will be implemented in PC-1D software, and it is built up by creating 4-layers of p-type background doping semiconductors, so each layer has its own characteristics. They are stacked in decreasing band gap order to guarantee efficient absorption of different wavelengths of the incoming light spectrum. The top layer is made of As, second layer is made of As, third is made of GaAs, and fourth bottom layer is made of Ge. The to three layers have lattice constants of 5.656Å, 5.653Å, and 5.646Å, respectively. Input parameters of each separate layer and optimal parameters of the overall simulated structure are presented in Tables (1) and (2).

Doping density is gradually decreased so that the field penetrates across the whole absorbing layers. The rear surface of the bottom Ge layer is diffused by p-type dopant (higher doping density of Ge with uniform doping profile) to construct a back-surface field layer which reduces surface recombination velocities. The resulted structure is shown in Figure 2.

Table (1) Input parameters used in the simulation

Layer	Band gap (eV)	Thickness (μm)	Back Doping (cm^{-3})	μ_n (cm^2/V$_s$)	μ_n (cm^2/V$_s$)
Al$_{0.95}$Ga$_{0.05}$As	2.148	0.5	5x	6246	316
Al$_{0.3}$Ga$_{0.7}$As	1.817	2.3	1x	6246	316
GaAs	1.424	7.1	1x	8569	408
Ge	0.664	12	1x	3895	2505

Table (2) Main parameters used in the simulation

Parameters	Values
Device area	250
Temperature	25°
Front surface texture angle	54.74°
Front surface texture depth	3 μm
Constant intensity	0.1 W
Spectrum	AM 1.5G
Voltage sweep	-0.8 to 0.8 V
Base contact	0.0015 Ω
Internal conductor	0.1 S
Thickness	31.9 μm
Excitation mode	Transient 100 steps
Exterior front reflectance	5%

4. SIMULATION AND RESULTS ANALYSIS

The simulation of a junction-less solar cell includes determining the generation and recombination of electrons and holes, energy band diagrams, electric field and the current_voltage (IV) curve. The IV curve is the most important output since it gives the most relevant parameters used to evaluate the performance of solar cells. The main parameters are solar cell efficiency, short circuit current, open circuit voltage. The coming graphs are measured with one SUN solar radiation.
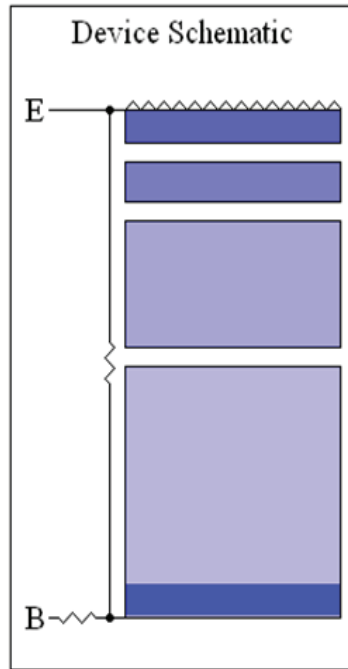
Figure 2. Simulated schematic of the Junction-less Solar Cell

A. *Energy Band diagram*.

Figure 3 represents a gradient in the band gaps due to efficient photon energy absorption by the subsequent layers of different band gap elements, where the top layer extracts energy from the highest energy photons while the subsequent layers absorb all remaining photons above its band gap.

B. Photo Generation and Carrier Recombination

It's obvious from the Figure 4 that the cumulative photo-generation of carriers continue to increase, while no significant carrier recombination is observed along the device till the rear surface of the bottom layer where the dopant dose is increased in order to create a back surface field layer to reduce the surface recombination velocity and hence control the flow of carriers.

As we mentioned earlier, the electric filed still the main contributor of the photovoltaic action. As shown in Figure 5, charge separating electrostatic fields exist at the transitions between layers. This charge separation action is the direct contribution of the electric field into the Voc.
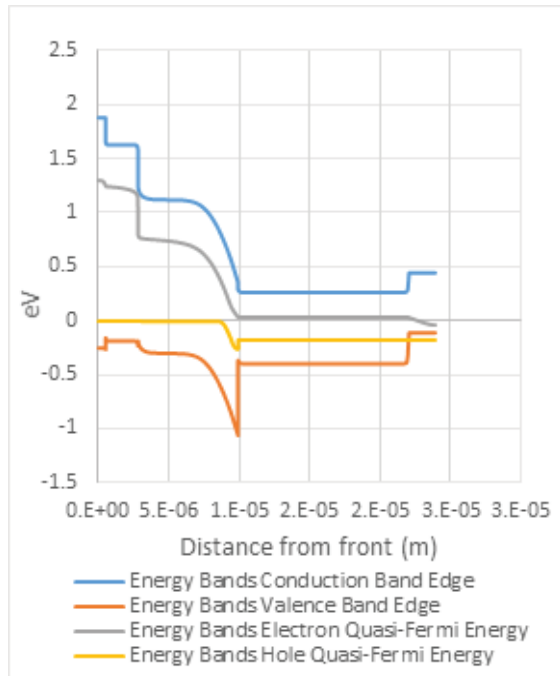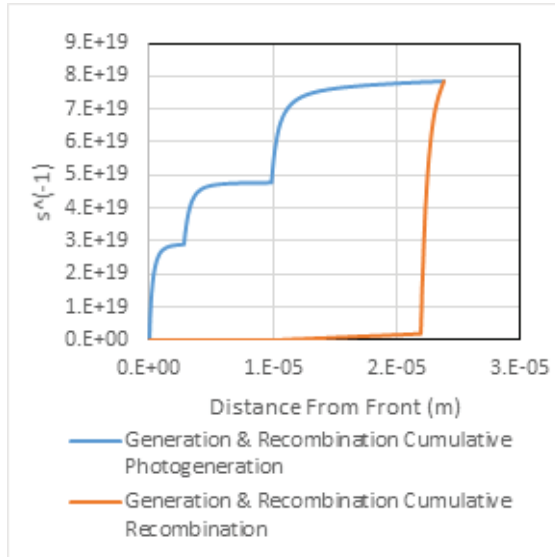
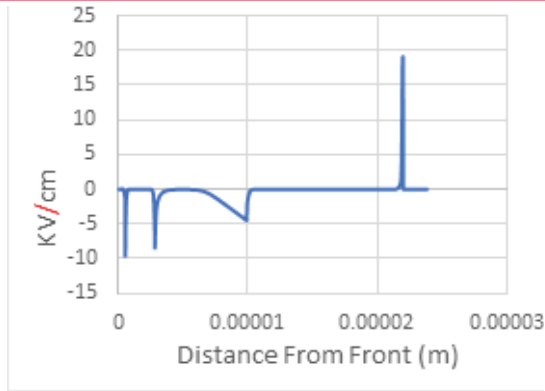**Figure 3: Energy Bands**

Figure 4: Generation & Recombination

Figure 5: Electric Field

C. Electric Field.

D. Voltage Versus Current and Power Curves.

It can obviously be seen from the Figure 6 that the device responds as any usual solar cell, which ensures that the constructed junction-less solar cell can actually produce the photovoltaic action.
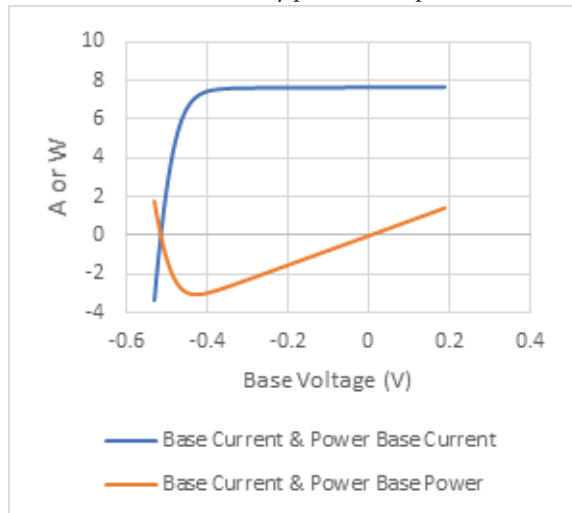

Figure 6. Base Current & Power

The performance of the proposed As /As /GaAs/Ge junction-less solar cell is shown in Table (3).

Table (3) Electrical parameters of the simulated junction-less solar cell

Electrical Parameters	Value
Short Circuit Current (mA/)	30.52
Open Circuit Voltage (V)	0.5135
Fill Factor (%)	77.62
Maximum Output Power (W)	3.041
Conversion efficiency (%)	12.164

5. CONCLUSIONS

It is proved through this paper that the diffusion of carriers (Dember effect) and effective forces arising from electron and hole affinity variations and band effective density of states variations are also possible sources of photovoltaic action rather than the pn-junction built-in electric field. Hence, even though the junction-less solar cell has low KPI's compared to existing conventional solar cells, but it actually behaves as a solar cell. Different device structures need to be investigated to enhance the performance of the proposed junction-less solar cell.

REFERENCES

[1]. *S.Parasuraman:Fundamentals of Electronic Materials and Devices https://drive.google.com/file/d/1DDunT6xdKZqb74 lWWEoPIUdzmYbM33W2/view*

[2]. *Adegbenro Ayodeji: Comparison Of Novel And State Of The Art Solar CellS, June 2016*

[3]. *R.W Miles and K. M. Hynes. Photovoltaic solar cells: An overview of state-of-the-art cell development and environmental issues. University of Northumbria. Newcastle, UK. November 2005.*

[4]. *Xiyang Cai, Xinjie Zhou, Ziyi Liu, Fengjing Jiang, Qingchun Yu: An in-depth analysis of the silicon solar cell key parameters' optimal magnitudes using PC1D simulations. Optik - International Journal for Light and Electron Optics, 27 February 2018.*

[5]. *Abubaker Ben Othman, Khaled M. Dadesh: Numerical modelling of solar cells structures, May 2003.*

[6]. *Preeti Jha, Vibha Tiwari: Design and degradation performance analysis of a 3 junction's solar cells using PC1D. International Journal of Advance Engineering and Research Development. Volume 5, Issue 05, May -2018.*

[7]. *Nordine Sahouane, Abdellatif Zerga: Optimization of antireflection multilayer for industrial crystalline silicon solar cells, 2014*

[8]. *Simon P. Philipps, Frank Dimroth and Andreas W. Bett: High Efficiency III–V Multijunction Solar Cells.,2013.*

[9]. *Zhaosheng Hu, Zhenhua Lin, Jie Su, Jincheng Zhang, Jingjing Chang: A Review on Energy Band-Gap Engineering for Perovskite Photovoltaics, September 2019*

[10]. *Stephen J. Fonash: Solar Cell Device Physics. Academic Press,1981.*

[11]. *Würfel, Uli, Andres Cuevas, and Peter Würfel. "Charge carrier separation in solar cells". IEEE Journal of Photovoltaics. January 2014.*